行政院國家科學委員會專題研究計畫成果期中報告

※※※※※※※※※※※※※※※※※※※※※※※※※

※奈米結構的量子電動力學及量子傳輸(2/3) ※

※※※※※※※※※※※※※※※※※※※※※※※※※

計畫類別：跨領域前瞻研究計劃(整合型)

計畫編號：NSC：92-2120-M-009-010

執行期間：92 年 12 月 01 日 至 93 年 12 月 31 日

計畫主持人：褚德三 (Der-San Chuu) –

共同主持人：林俊源、朱仲夏、許世英、趙天生

本成果報告包括以下應繳交之附件：

執行單位：國立交通大學電子物理系

中 華 民 國 93 年 05 月 29 日

Cavity QED and quantum transport in nanostrucrures

奈米結構的空腔量子電動力學及量子傳輸現象之研究

總執行期限：2002/08/01 ~20005/12/31

PI：Der-San Chuu（褚德三），交通大學電子物理系，dschuu@cc.nctu.edu.tw
Co-PI：C.S.Chu (朱仲夏)；S.Y.Hsu (許世英)；T.S.Chao (趟天生)；J.Y.Juang (莊振益)；J.Y.Lin (林俊源)

(1). 子題一：奈米結構中之超輻射現象

1.Experimental part：

We have measured the relaxation dynamics of photoexcited carriers and the lifetime of photoluminescence in semiconductor nanostructures by the time-resolved spectroscopy. Experimental data show that the relaxation dynamics of photoexcited carriers in the sample with single quantum well (QW) is significant different from the sample with several quantum wells and their lifetime of photoluminescence are also distinct. For further analyses, we could extract the phenomena of superradiant excitons from the time-resolved spectroscopy. Additionally, we are building a spectrum analyzer with spatial and temporal resolution, which are < 20 nm and < 100 ps, respectively. So far it has been successfully tested in quantum dots sample at room temperature.

透過時間解析光譜之量測，我們可以直接觀察量子井或量子點中光激載子之弛緩動力行為以及所產生螢光之生命期。實驗結果顯示，單層量子井之光激載子之弛緩動力行為與數層量子井有很大的差別，同時產生之螢光生命期也較短大約 0.54 ns。至於是否為所預期之超輻射現象，需要更進一步的分析研究。此外我們正積極建構一套具有空間解析及時間解析之光譜量測系統，目前已在室溫的量子點樣品上測試成功，空間及時間解析能力分別為< 20 nm 和 < 100 ps。

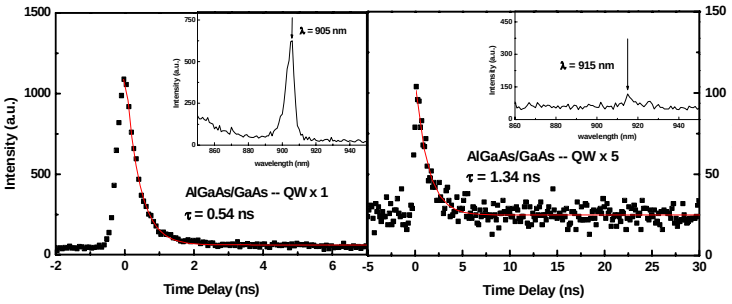

Time-resolved PL

The time-resolved photoluminescence of GaAs/AlGaAs QW sample with single layer and five layers were measured at 15 K. The lifetime of single layer QW is smaller than that of five layers QW.

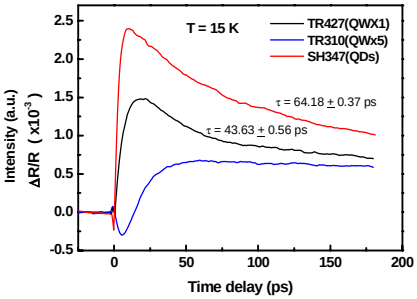

Pump-probe Measurements

The transient reflectivity change of GaAs/AlGaAs QW sample with single layer, five layers, and GaAs/InGaAs quantum dots (QD) at 15K.

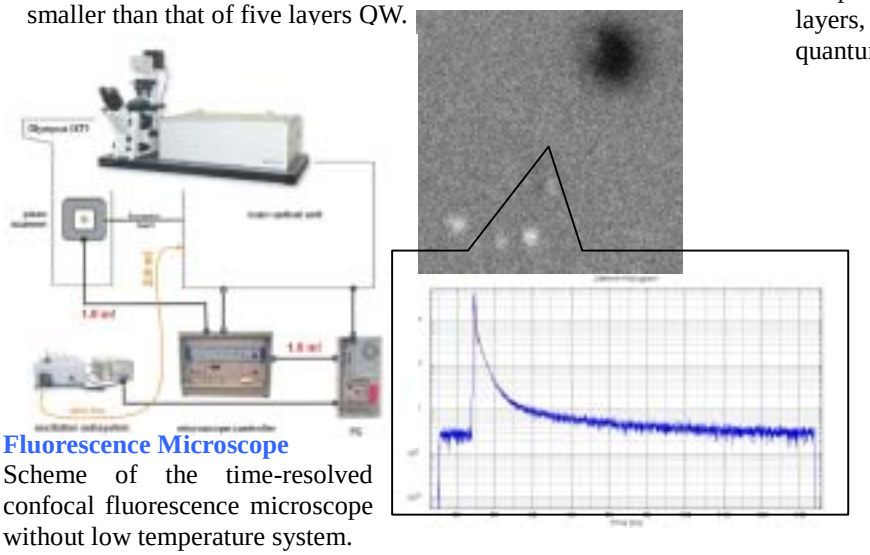

Fluorescence Microscope

Scheme of the time-resolved confocal fluorescence microscope without low temperature system.

2D PL image and lifetime

The 2D photoluminescence image of QDs with resolution of 67 nm per pixel over the 10 μm x 10 μm scanned area. The local PL lifetime was measured by the XY -scanning piezo stage and time - resolved confocal fluorescence microscope at 300K.

2. Theoretical part

On the theoretical side, we have successfully worked out the radiative properties of low-dimensional (quantum wire and quantum ring) excitons. Renormalized frequency shift in quantum wire and Aharonov-Bohm effect in quantum ring maybe observable in optical measurements. Furthermore, shot noise spectrum of superradiant entangled excitons in double dots is also investigated thoroughly. We predicted that entanglement can be read out by means of current noise and its value is enhanced by a factor of two.

在理論部分，我們已經成功的計算出量子線與量子環激子的輻射性質，尤其是量子線激子的重整化頻率遷移以及量子環激子的 Aharonov-Bohm 效應都有可能從光學實驗去驗證。除此之外，我們也計算出雙量子點中糾纏態激子的 shot-noise spectrum，理論的結果顯示量子糾纏態可藉由 noise spectrum 來讀取，而其值會是古典值的兩倍。這些結果都將發表在今年(2004)的 Phys. Rev. B., Phys. Lett. A.及 Solid. State. Communications.

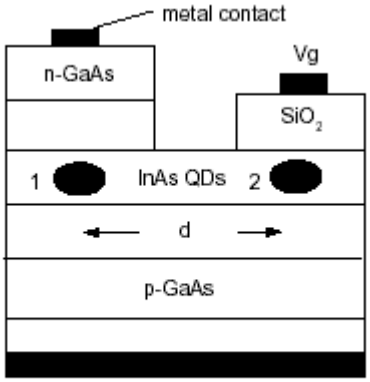

FIG. 1: Schematic view of the structure.

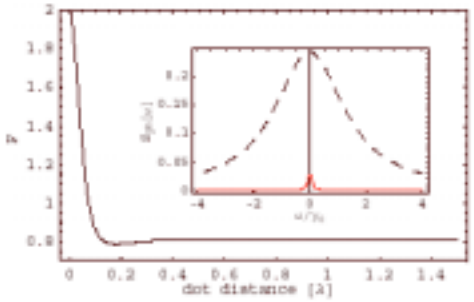

FIG. 2: Fano factor as a function of inter-dot distance. The vertical and horizontal units are $\frac{S_{ph}(0)}{\frac{2\Gamma_0}{\pi}}$ and λ, respectively. The inset shows the value of $S_{ph}(\omega)$ is equal to that of one-dot limit for $d \to \infty$ (dashed line), while it approaches zero noise as $d = 0.005\lambda$ (red line).

Papers to be published:

■ Review Articles (Invited)

Effects of cavity and superradiance on electrical transport through quantum dots, Progress in Quantum Dot Research **(Nova Publisher, 2004), Chen YN, Chuu DS, T. Brandes**

■ Journals

1. Shot noise spectrum of superradiant entangled excitons,
   Accepted, **Phys. Rev. B.** (2004), Chen YN, T. Brandes, Li CM, and Chuu DS.
2. Superradiant and Aharonov-Bohm effect for the quantum ring exciton,
   Solid State Commun. 130, 491 (2004), Chen YN and Chuu DS.
3. Renormalized frequency shift of a Wannier exciton in a one-dimensional system,
   Phys. Lett. A 324, 86 (2004), Chen YN and Chuu DS.
4. Current induced entanglement of double quantum dot excitons,
   Accepted, **International journal of nanoscience** (2004), Chen YN and Chuu DS.

3. Sample fabrication

The goal of this sub-project was to fabricate the process of tunneling junction. The experimental equipments, such as e- beam lithography etc., supported by NDL were used to fabricate devices with ultra short channel (< 100nm) and thin dielectric layer (< 2.0nm). Our goal was to measure quantum effects at high temperature after devices fabrication, and study quantum effects from the different device structures. To fabricate different tunneling junction structures by E- beam lithography, which could work at high temperature. In the first stage, we have finished the layout by the software of L-edit (The attached figures are the device structures), and the process flow was defined. The manufacturing machines, like the E-beam, PVD, PECVD etc, were needed. The process was now after the first layer deposition of Al. In the next step, we will test the thickness of AlO_X and the etching rate of Al.

本子計畫之目的是執行總計畫在 Tunneling Junction 的製程部分。實驗設備系利用國家奈米元件實驗室的電子束微影系統等設備來進行本子計畫的的製程。目標是能夠製作出極小線寬（＜100nm）和極薄絕緣層厚度（＜2.0nm）的元件。希望能夠在元件作完成後可以在高溫下和不同的結構下量到量子現象，並且可以研究各種不同的物理現象。

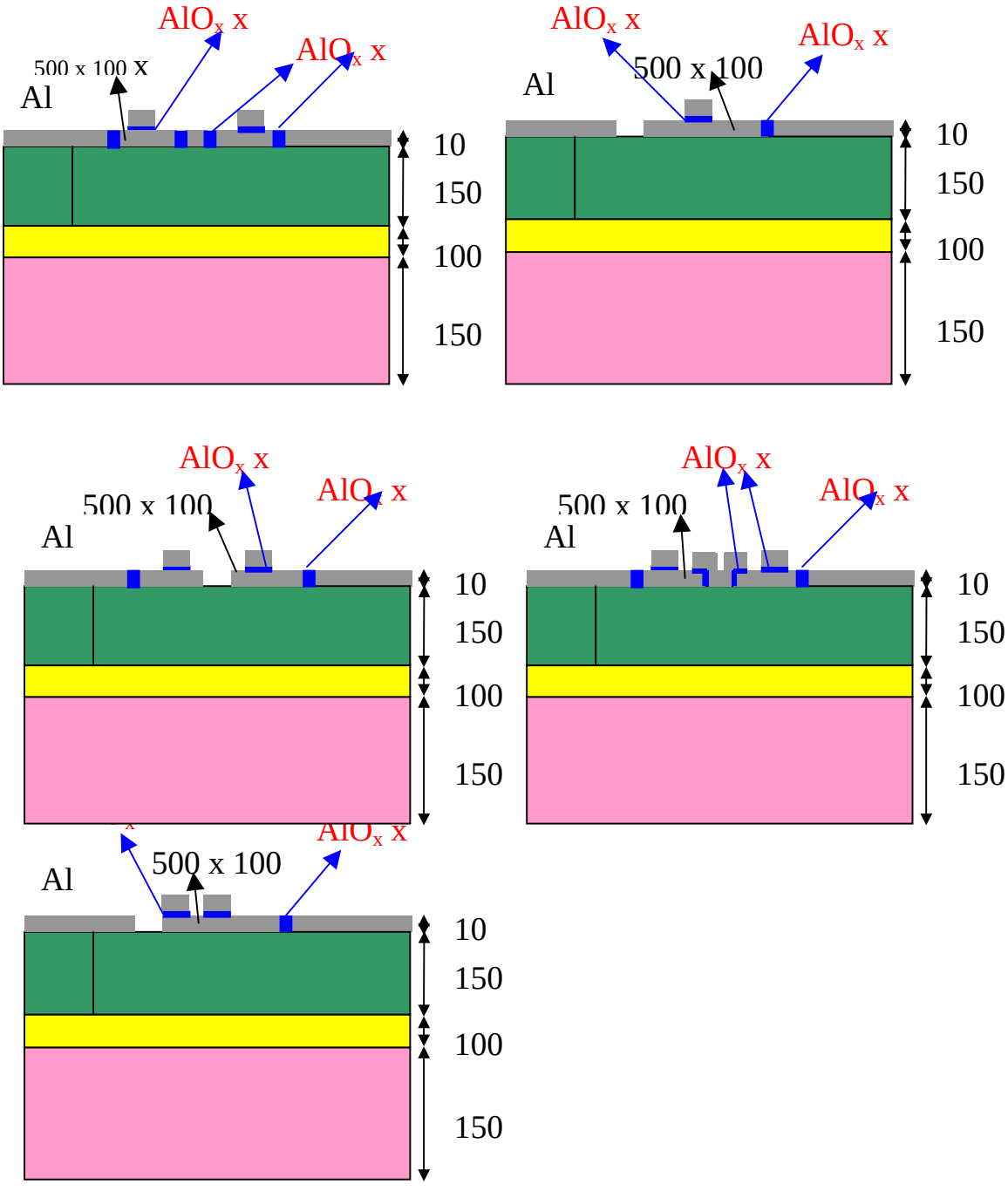

(1). 子題二:可調式奈米結構的電性與光致電性研究

(A). We consider an experimental configuration for dc spin current (SC) in a quantum channel in the presence of Rashba spin-orbit interaction (SOI). The configuration involves only one ac-biased finger-gate (FG) that locates atop and orients transversely to the quantum channel resulting in the generation of the dc spin current. No dc charge current, however, is generated by this spin-pumping configuration. Our study also shows that the spin current generation can be enhanced significantly in a double finger-gate configuration.

我們在有 Rashba 自旋軌道交互作用的量子窄通道中外加一個有時變場的指狀閘極結構來產生直流自旋電子流;然而這種結構並不會產生淨電荷流;我們研究發現可以利用一對指狀閘極結構有效率的增加自旋電流的大小。

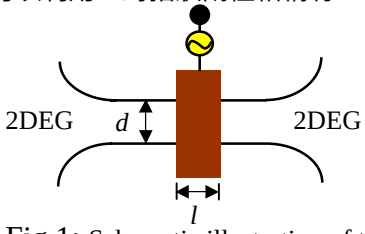

Fig.1: Schematic illustration of the setup for the generation of dc SC.

[Results and discussions]:

1. A spin-resolved driving electric field, which is induced by the ac-biased FG, resulting in generation of a dc SC.
2. The dip feature at $\mu/\Omega=1$ indicates the electron emitting one energy quantum $\hbar\Omega$ making intersideband transitions to the subband threshold forming a spin-resolved quasi-bound -state (Figs. 2 (a)-(c)). Other parameters: $\alpha_0=0.13$ $(3\times10^{-11}\text{eVm}/\hbar)$, the FG width $l=80nm$, and external frequency $\Omega=28GHz$.
3. The SC is enhanced when we increase the dynamic Rashba SOI coupling constant α_1 by tuning the gate voltage (Fig. 2 (d)).
4. Our results also show that the pumping spin per cycle $N_P^s=(2\pi/e\Omega)\left|I_R^{\uparrow}\right|$ would be enhanced efficiently in the double finger-gate case (Fig. 3). Other parameters are chosen: $\alpha_0=0.13$, $\alpha_1=0.065$ the FG width $l=88nm$, the double FG's separation distance $\Delta l=88nm$ and the external frequency $\Omega=14GHz$.

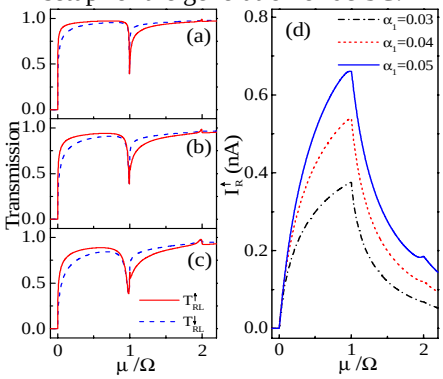

Fig.2: Spin-resolved transmission as a function of μ/Ω in various (a) α_1=0.03, (b) 0.04, and (c) 0.05. Fig. 2 (d) shows the SC in above cases.

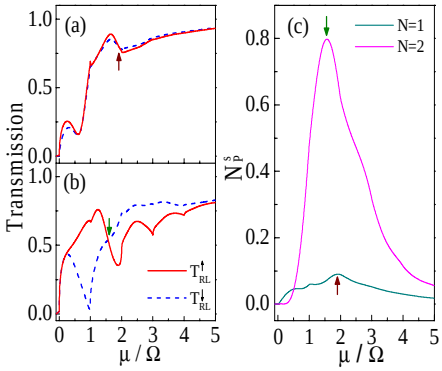

Fig.3: Spin-resolved transmission as a function of μ/Ω in FG number : (a) $N=1$ and (b) $N=2$. The N_P^s is plotted as a function of μ/Ω.

[Conclusion]:

In conclusion, the ac-biased FG generates a spin-resolved driving force leading to the pure SC generation, without accompanying any charge current. For $N=1$ case, the SC is enhanced in the larger α_1. The sufficient condition for generation of dc SC is that there are both of the static and dynamic Rashba coupling constants in this system. In addition, it has shown that the double -FG is already enough to enhance the dc SC efficiently.

Finger-gate array quantum pumps: pumping characteristics and mechanisms

(B). We propose an experimental configuration for nonadiabatic quantum pumping in a narrow constriction. The pumping potential is generated by ac biasing a pair of finger gate arrays (FGA). Pumping of charges is caused both by the mechanism of time-dependent Bragg reflections, and by the breaking of the electron transmission symmetry when the pumping potential is predominately of a propagating type. This propagating wave condition can be achieved both by an appropriate choice of the FGA configuration and by the monitoring of a phase difference ϕ between the ac biases in the two FGAs.

我們建議在窄結構中利用一種非緩變機制來產生量子幫浦效應,電荷幫浦機制是由於與時間相關的布拉格反射以及電子穿透的對稱性被破壞所造成的;我們可以調制指狀閘極陣列結構以及閘極間的相位變化來達到傳導電子波的條件。

[Results and discussions]:

1. For single pair $N=1$, the pumped currents versus $X_\mu = \mu/\Delta\varepsilon + 1/2$ for external frequency $\Omega \approx 18GHz$ (solid curve) and $\Omega \approx 3GHz$ (dashed curve) are plotted in Fig.2. (μ is the incident energy and subband level spacing $\Delta\varepsilon \approx 0.13meV$). Other parameters are chosen: $\phi = \pi/2, \delta x = \alpha d, \alpha = 1/4$.

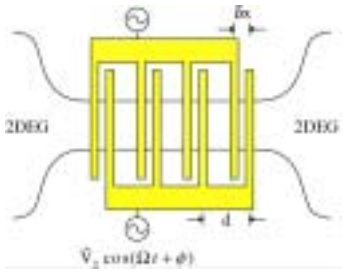

Fig.1:Top view of the proposed system structure for the case of pair number $N=4$

2. For $N=4$ case, the pumped currents versus X_μ for external frequency $\Omega \approx 18GHz$ (solid curve) and $\Omega \approx 3GHz$ (dashed curve) are plotted in Fig.3. Other parameters are chosen: $\phi = \pi/2, \alpha = 1/4$. The peaks have flat tops for the solid curves due to nonadiabatic pumping mechanism. Another important mechanism is the time-dependent Bragg reflection in the case of $N=4$. In the case of $\Omega \approx 3GHz$, the energy gap is at best only partially opened, as we see from the nonzero transmission, because we have only $N=4$ FG pairs. Thus our result shows that the condition of occurrence of the of adiabatic-pumping is less stringent than we would have expected originally.

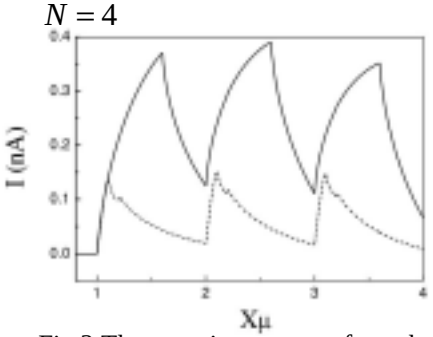

Fig.3:The pumping currents for the case of pair number $N=1$.

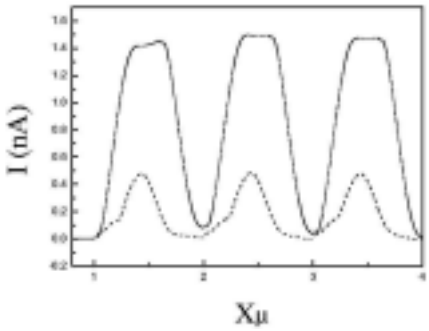

Fig.4:The pumping currents for the case of pair number $N=4$.

[Conclusion]:

In conclusion, we have proposed a finger-gate array pair configuration for the generation of quantum charge pumping. The robustness of the time-dependent Bragg reflection in QPC has been demonstrated, and the pumping mechanism is understood.

(c).奈米結構之高頻量子傳輸頻譜之實驗部份

一、背景與理論

早期，Thouless[1] 認為在一維系統的閘極上控制一隨時緩變的電位，將產生電子傳輸的抽運機制，形成電流。直到 1999，Marcus[2] 實驗小組在閘極局域的量子點系統，藉由兩有相位差的同步交流高頻（1~16MHz）電位調製，始觀察到這電荷抽運現象。其元件設計如圖（一）所示：利用紅點所標示的三閘極給予負偏壓使下層的二維電子系統形成約<~μm^2 的量子點，另二閘極則作為 AC 電位控制，如圖所示之間有一相位ϕ（0~2π）的調控，

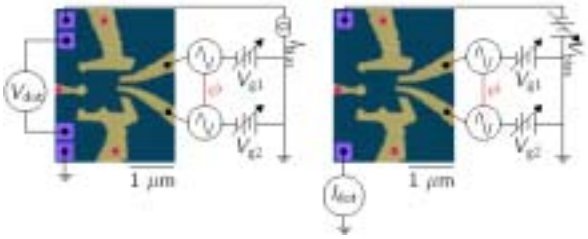

Figure 1. 量子點的設計與測量模組[3]，左圖：觀測抽運造成的 source-drain 電位(I_{bias}=0)；右圖：觀測抽運造成的 source-drain 電流(V_{bias}=0)

在左圖的實驗組態下，觀察到抽運導致了 sub-μV 電壓且 $V_{dot} \propto \sin\phi$，這被稱為十字轉門抽運（turnstile pump）。一般以雙振盪位障機制解釋，藉由 chemical potential 的先降使得量子點有一空的低能態容許載子進入，之後又調升 chemical potential 使載子離開至另一端；所以兩控制的 AC 電壓有$\pi/2$ 相位差可得最大的 V_{dot}。另外，Altshuler 等認為彈道區域的波量子干涉機制應被重視 [4]；最近朱仲夏等提出在彈道式窄通道的 Non-adiabatic 量子抽運理論 [5]，藉由空間與時間的週期調變，$V(x,t) = V_o \cos(Kx - \Omega t)\theta(\frac{L}{2} - |x|)$，（x 為 source-drain 方向）預期也可觀察到 non-adiabatic 抽運傳輸，也就是在二維電子系統先以 Split gates 加負偏壓形成一維窄通道，之後再其上端的所謂 finer gates 加 AC 電場（如圖二所示的提議實驗組態），並預期可從實驗數據定量分析（頻率、相位、finger gate 的空間不對稱等造成抽運電流相對變化）更瞭解傳輸電子的同調非彈性散射機制（coherent inelastic scattering）。

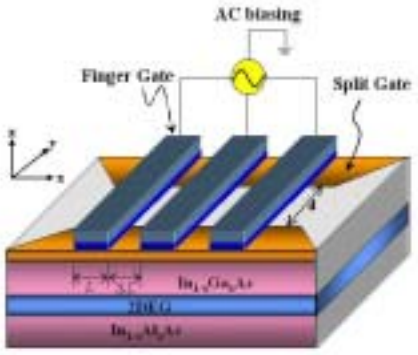

Figure 2. The experimental structures of a spin-polarized current generator device due to the spin-orbit interaction (SOI)[6].

二、實驗方法

去年（2003）九月我們購置電子束微影圖形產生軟體，在自我組裝於同年一月份購置的 Hitachi 掃描電子顯微鏡系統，目前系統已相當完備，間距與線寬可控制於 75nm±10nm，對於初學者能以簡單型的 filament-type SEM 完成如此微小與精準元件設計，真是如釋重負。

本子計畫乃研究奈米結構的抽運傳輸機制，因此在高 mobility 的二維電子系統製作微結構的量子元件為首要任務；我們延伸 Marcus 小組的設計，也想藉由量子點尺寸掌控 level spacing，能更深入探討此系統的抽運機制。

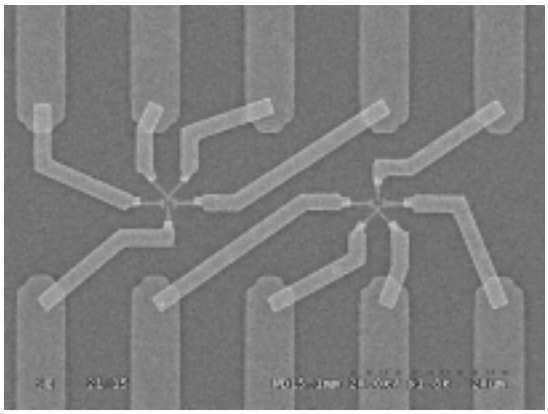

Figure 3. SEM image of two quantum dot systems.

.

圖三展示在一元件內製作的二量子點，其金屬閘極從 0.25mm×0.25mm 的打線點經光微影與電子束微影等多道製程，連接至μm^2 的 Dots。圖四為更高倍率的放大 Dot 結構圖，上圖類似 Marcus 小組設計，兩支 AC 閘極緊鄰一邊，而下圖乃將兩支分置左右兩邊。

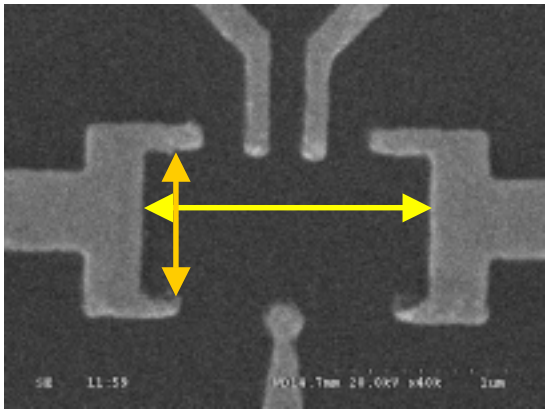

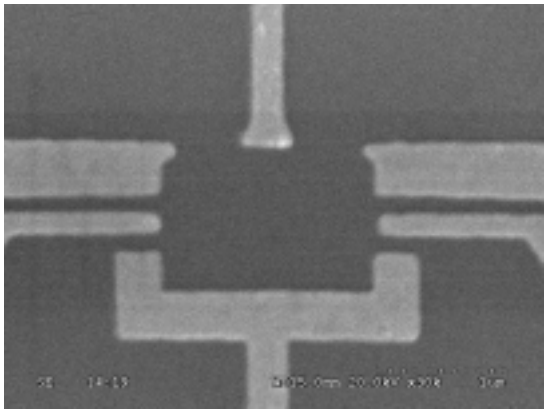

Figure 4. Two SEM images of a quantum dot system with different arrangement of AC pumping gates. (Top) Two AC pumping gates are next to each other. (Bottom) Two AC gates are at the opposite sides.

除此之外，我們也針對本小組朱仲夏老師提案製作不同 top layer 的 finger gate 組態，

其中困難性在於: (1)split gate 與 finger gate 之間的絕緣層不可有漏電，(2)由於電子平均自由徑約為 10μm，split gate 寬度有限，造成上層的 finger gate 在多對形況下相當擁擠，proximity effect 增添製作難度。我們採用 Pepper 小組的方法以 PMMA 曝於電子劑量下，可形成約 120nm 絕緣層，在室溫時其電阻大於 GΩ(跨 split and finger gates 測量)，因此在低溫的漏電率更低，因可忽略。圖五為此元件的 SEM 影像圖，正中間 25μm×25μm 的深黑色區即為絕緣 PMMA 層，在其下方有對 split gate（中間 0.3μm 間隙），而上方有數對微細交錯 finger gates（跨過 0.3μm 間隙），並以二支較粗的 metal gates 連接得以分別控制 AC 電場的時變因子。理論推算由空間的不對稱性，在無相位差下也可有抽運傳輸，因此我們對不同對的 finger gate 可作一系列對偶（等距）與不對稱（不等距）的設計。

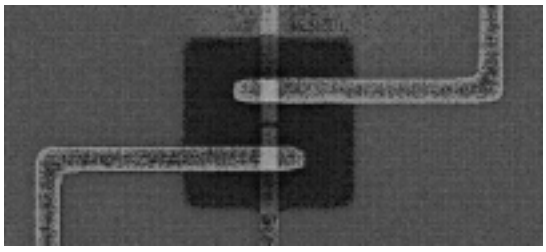

Figure5. SEM image of 2DEG with split gates and finger gates. A PMMA insulating layer（dark area）is sandwiched by these two layers.

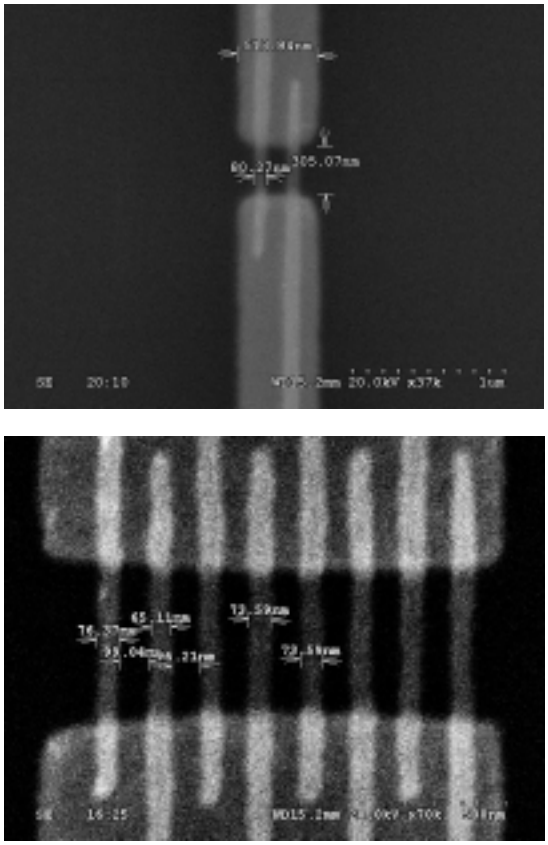

Figure 6. SEM images of narrow channels with different arrangements of finger gates. (Top) One pair of finger gate. (Bottom) Four pairs of finger gate.

圖六顯示二種不同的組態。由於線寬僅止於 70±10nm，因此當對數增加時，split gate 寬度大約需長 1.2μm，由於以色列 Braun center of Submicron Research 的 Dr.Umansky 給的 2DEG，mean free path ℓ~7.5μm(經 Subnikov-deHaas 振盪的 $R_{xx}(H)$ 與 Hall effect $R_{xy}(H)$測量)，我們得知 long channel 將造成一些 scattering 模糊其窄通道的量子傳輸，因此盡可能避免通道長度大於 1.5μm。

在同高頻但具相位差的兩訊號產生設備設置，由學校配合款項支援購置 Agilent E8257C(250kHz~40GHz) source generator, 另配合系上原有 HP8752C network analyzer(250kHz~1.3GHz)，我們可製造兩相位差高頻同調訊號(250kHz~1.3GHz，phase difference ϕ can be continuously changed from -2π to 2π)。原 0.3K 低溫系統成功地加設置兩 SMA 端子，銜接的兩同軸電纜線獨立地經過完善 heat sink 安排連接樣品台上樣品的 finger gates。

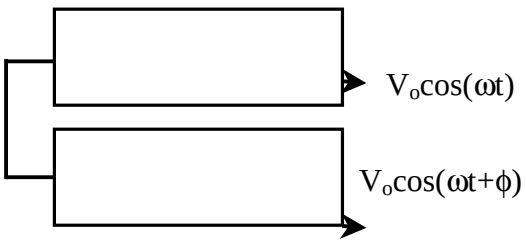

Figure 7. Experimental setup for two high frequency sources with same frequency and different phases.

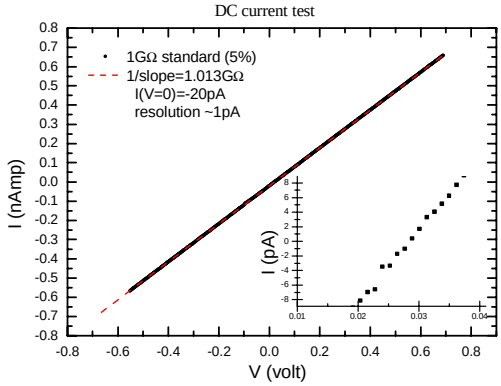

Figure 8. DC current resolution test result for our measurement system.

三、實驗數據與討論

目前使用的二維電子系統為 MBE 長成的 GaAs/$Ga_{1-x}Al_xAs$ 異質結構，其結構如圖九，2DEG 在離表面 93nm 下方。

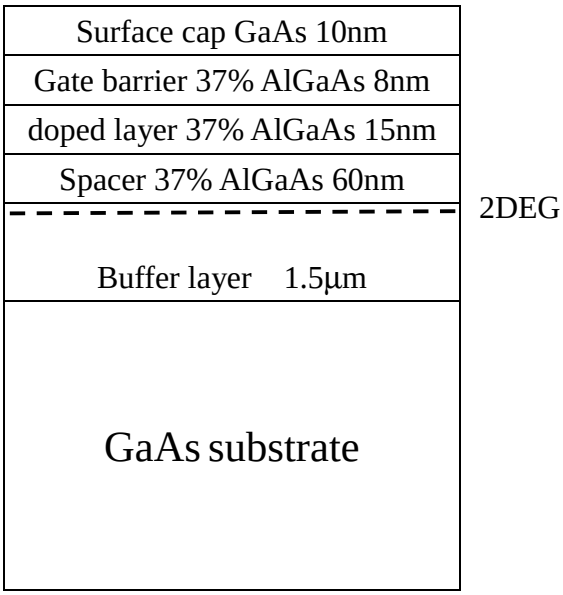

Figure 9. Schematic diagram of a GaAs/AlGaAs heterostructure.

其橫向傳輸 $R_{xx}(H)$ 展現由磁場所引起的 Landau level quantization 及在 2DEG. 中的 step-like density of states 之典型的 Subnikov-deHaas 振盪，利用此振盪週期，可得樣品的 carrier concentration.

$$n_s = \frac{2e}{h}\frac{1}{\Delta(1/H)}$$

Hall resistance R_{xy}(H)也顯示出對應於 R_{xx}=0 的平臺。甚至在很弱磁場中我們亦可解析出這些平臺， Carrier concentration 也可用 Hall measurement.計算出；從兩者測量得出相同結果：$n=1.2\times10^{11}/cm^2$.樣品之 mobility 為 $1\times10^6 cm^2/Vs$.。略低於 Dr.Umansky 給的樣品數據 $n=1.4\times10^{11}/cm^2$、 $\mu=2.2\times10^6 cm^2/Vs$ (w/o. illumination)。

在解決歐姆接點等問題後，contact 電阻可控制於 100Ω左右，樣品於低溫下的方塊電阻值應為數十Ω，我們先著重於量子窄通道的傳輸性質測量，split gate 上加負偏壓使 2DEG 因負電位之 depletion 限制電子運動區域。當 sweeping gate voltage V_g,電子通道寬度即縮減，故我們可觀察到系統由二維至準一維、甚至通道完全封閉 (pinch off)的傳輸行為。我們測量數個不同閘極縫隙寬 d_{gap} 與不同通道長度$\ell_{channel}$ 的元件，

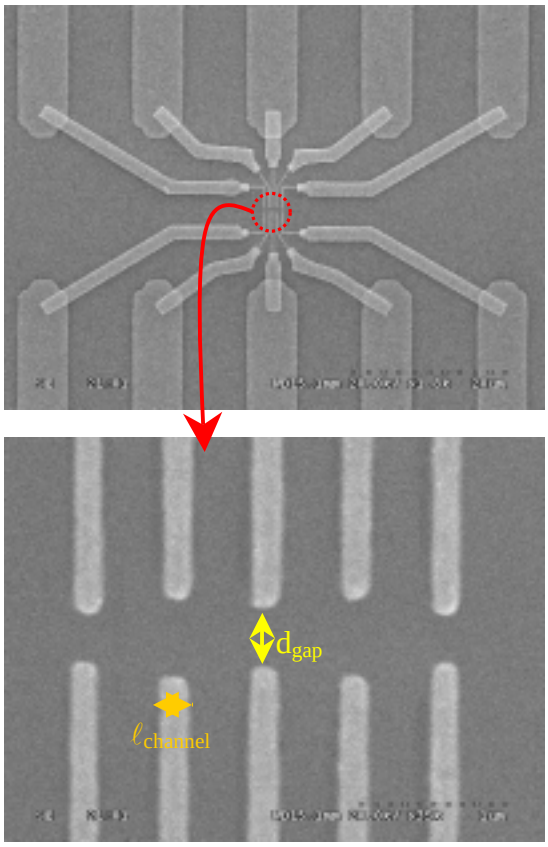

Figure 10. SEM images of narrow channels with different arrangements of split gates.

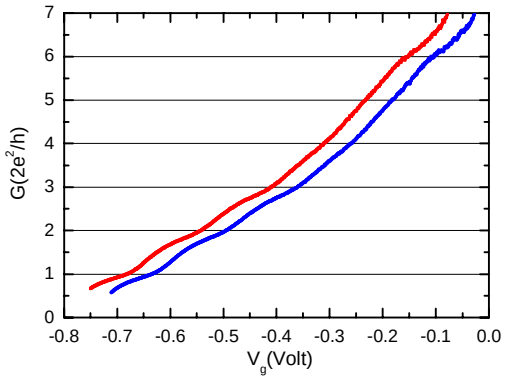

Figure11. Two quantized conductance vs. V_g for two devices with identical split gate arrangements, d_{gap}=400nm, at T=0.32K. Blue data is shifted by +0.05V for clarity.

圖十一展現典型的電導平台，$G = N\frac{2e^2}{h}$ （N∈Z），電子的傳輸從二維行為（V_g>-0.05V and R_{sheet}=constant~60Ω），在當 V_g~-0.05V 時，93nm 下的通道始受 split gate 的 depletion 變窄，傳輸成似一維行為，而後開始展現一維的平台電導；我們發現若在同一樣品上，有不同 d_{gap} 的通道，發生二維到似一維行為轉變的 V_g 大致相同，但可觀察到的平台數隨著 d_{gap} 的減小而變少，d_{gap}=600nm 則平台數可為 14、d_{gap}=400nm 則平台數為 8 、d_{gap}=200nm 則平台數降為 4。這可以一維窄通道的量子傳輸加 V_g 與 d_{gap} 對通道寬度影響的考量而理解；另雖然 mean free path ℓ~10μm，但通道長度 $\ell_{channel}$ 約為 1μm 時，仍有一些散射機制會模糊化平台。

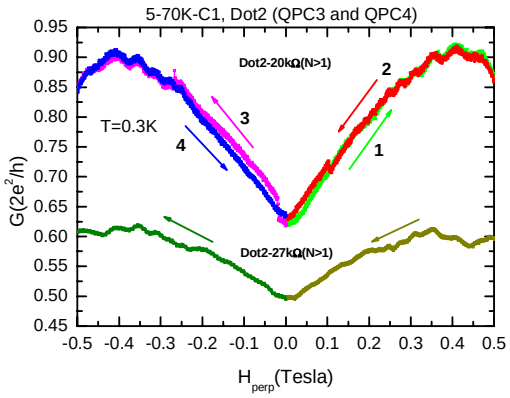

Figure12. Channel conductance vs. H for different V_g at T=0.31K. H is perpendicular to the 2DEG film plane and d_{gap}=400nm.

窄通道電性傳輸在磁場下的行為，與二維展現的典型的 Subnikov-deHaas 振盪有何不同，圖十二為窄通道的磁電導變化，在弱磁場下，窄通道的形成造成樣品的電導遠小於二維樣品（數百倍），但磁組似乎展現類似徵象，負磁組背景（H<0.4T）與電導振盪，我們目前正更深入釐清之間關係。

過去的一年半載，組裝完成整個奈米圖形的製程（含濕式蝕刻與電極製作），

也先從窄通道與量子點的特性測量來認識這些奈米元件，同步也完成 pumping pattern 的製作與高頻量測的架設，因此有關量子點與窄通道的 AC 抽運機制研究將即刻進行測量，相信短時間就會有所成果，由去年相關文章的論述[7]，不難發現由於實驗數據的缺乏，很多針對不同設計元件的 AC 抽運理論無法得到應證。

參考文獻

1. D.J. Thouless, Phys. Rev. B**27**, 6983 (1983).
2. M. Switkes, C. M. Marcus, K.Campman, and A.C. Gossard, Science **283**, 1905 (1999).
3. M. Switkes, Ph.D. thesis, Stanford University (USA), 1999.
4. F. Zhou, B. Spivak, and B. Altshuler, Phys. Rev. Lett. **82**, 608 (1999).
5. C.S. Tang and C.S. Chu, Solid State Commun. **120**, 353 (2001).
6. I. Tralle, Physica E**9**, 275 (2001).
7. M. Moskatlets and M. Buttiker, Phys. Rev. B**68**, 16311 (2003); D. Cohen, ibid **68**, 155303 (2003).